Inorganic Chemistry

Article

pubs.acs.org/IC

Light-Driven Hydrogen Evolution by BODIPY-Sensitized Cobaloxime Catalysts

Juergen Bartelmess, Aaron J. Francis, Karim A. El Roz, Felix N. Castellano, Walter W. Weare,* and Roger D. Sommer

Department of Chemistry, North Carolina State University, Campus Box 8204, Raleigh, North Carolina 27695-8204, United States

Supporting Information

ABSTRACT: We report four photocatalytically active cobaloxime complexes for light-driven hydrogen evolution. The cobaloxime catalysts are sensitized by different *meso*-pyridyl boron dipyrromethene (BODIPY) chromophores, bearing either two bromo- or iodo-substituents on the BODIPY core. The pyridine linker between the BODIPY and cobaloxime is further modified by a methyl substituent on the pyridine, influencing the stability and electronic properties of the cobaloxime catalyst and thus the photocatalytic efficiency of each system. Four cobaloxime catalyst complexes and three novel BODIPY chromophores are synthesized and characterized by absorption, fluorescence, infrared (IR) and nuclear magnetic resonance (NMR) spectroscopy, mass spectrometry, and electrochemistry. Crystal structures for the BODIPY−cobaloxime complexes **2** and **3** are presented. In contrast to the photocatalytically inactive, nonhalogenated reference complex **1**, the four newly reported molecules are active for photocatalytic hydrogen evolution, with a maximum turnover number (TON) of 30.9 mol equiv of H_2 per catalyst for the *meso*-methylpyridyl 2,6-diiodo BODIPY-sensitized cobaloxime complex **5**. We conclude that accessing the photoexcited triplet state of the BODIPY chromophore by introducing heavy atoms (i.e., bromine or iodine) is necessary for efficient electron transfer in this system, enabling catalytic hydrogen generation. In addition, relatively electron-donating pyridyl linkers improve the stability of the complex, increasing the overall TON for hydrogen production.

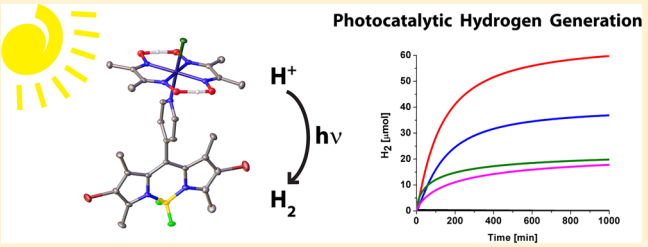

INTRODUCTION

Generation of fuels by harvesting solar energy is widely recognized as key technology for fulfilling the future energy needs of mankind.[1−3] Toward this, water-splitting approaches based on cobalt have drawn broad attention,[4,5] especially since cobalt is a relatively inexpensive, Earth-abundant metal, when compared to photocatalytic systems that incorporate expensive noble metals.[6−9] For proton reduction, e.g., hydrogen production, cobaloxime-based molecules are reported in several studies.[5,10,11] These include combinations of cobaloxime water reduction catalysts with a variety of different chromophores as photosensitizers, such as $Ru(bpy)_3^{2+}$ (as an early example from 1983),[12] Pt terpyridyl acetylides,[13,14] xanthene dyes,[15−17] perylene dyes,[18] tetrapyrrolemacrocycles,[19−24] or other metal complexes, such as $[Cu(dsbtmp)_2]^+$ (dsbtmp = 2,9-di(*sec*-butyl)-3,4,7,8-tetramethyl-1,10-phenanthroline).[25] While the $Ru(bpy)_3^{2+}$, Pt terpyridyl acetylide, $[Cu(dsbtmp)_2]^+$, xanthene dye, and some porphyrin-based systems[19,21,22,24] show catalytic hydrogen generation, others do not.[18,20] In combination with Ru-sensitized TiO_2 nanoparticles or carbon nanotubes, cobaloxime complexes have been shown to be efficient catalysts for the generation of hydrogen.[26,27] The mechanistic and electronic properties leading to the successful combination of a dye and a cobaloxime catalyst remain an area of active research.

Recently, we reported the synthesis and properties of a series of cobaloxime complexes covalently linked to *meso*-pyridyl boron dipyrromethene (BODIPY) photosensitizers.[28] BODIPY derivatives are well-known as photochemical active compounds for various applications.[29−35] Although hydrogen evolution in such BODIPY-sensitized molecules is substoichiometric,[28,36] we demonstrated that the introduction of either electron-withdrawing or electron-donating substituents on the pyridine linker alters the stability and redox potentials of the resulting BODIPY−cobaloxime complexes.[28] Earlier studies have proposed different mechanisms for the light-driven as well as for the electrocatalytic generation of hydrogen by cobaloxime complexes. Each proposed mechanism involves multiple electron transfer steps.[10,14,37−39] It can be concluded that these initial electron transfer steps are crucial for the realization of catalytic hydrogen generation of dye-sensitized cobaloxime complexes. In the present study, we report a convenient and effective method for modifying BODIPY-sensitized complexes.[29,30] The introduction of halogen substituents in the 2 and 6 position of the BODIPY core (see Scheme 1 for numbering) is reported to significantly shift the oxidation and reduction potentials to lower values.[40] In addition to these tunable redox potentials, the incorporation of heavy atoms such as bromine or iodine is known to quench BODIPY fluorescence

Received: January 28, 2014
Published: April 11, 2014

   dx.doi.org/10.1021/ic500218q | *Inorg. Chem.* 2014, 53, 4527−4534

Scheme 1. Numbering of a BODIPY Molecule

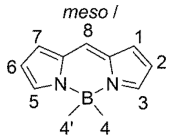

and leads to the formation of photoexcited triplet states in high quantum yield.[29,41,42]

Brominated and iodinated BODIPY derivatives, in combination with platinized TiO_2 as a catalyst, have shown to be effective for solar hydrogen production.[43] Transient absorption studies of the aforementioned photocatalytic systems suggest triplet-state electron transfer from the photoexcited BODIPY to the catalyst. Based on these findings and earlier studies of other cobaloxime-based photocatalysts for light-driven hydrogen generation, a long-lived, high yield triplet excited state is necessary for an efficient photocatalytic process.[15]

In this paper, we report, for the first time, light-driven catalytic hydrogen evolution of BODIPY-sensitized cobaloxime complexes. The 2,6-dibromo BODIPY and 2,6-diiodo BODIPY[44] derivatives and their corresponding cobaloxime complexes are reported. In addition, we study the influence of a relatively electron-donating methyl substituent on the pyridine linker on photocatalytic hydrogen generation efficiency. This modification of the spacer is known to lead to a shift in the catalytically relevant Co centered redox couples to lower potentials and improves stability in the resulting complexes, because of increased basicity of the pyridine.[28]

EXPERIMENTAL SECTION

General Procedures. Triethylamine, *N*-bromosuccinimide, and iodic acid were purchased from Alfa Aesar, and elemental iodine was obtained from Fisher Scientific. All solvents were ACS grade and used as received, unless otherwise noted. Reactions and measurements were carried out under ambient conditions, unless otherwise noted. Deuterated chloroform and dichloromethane (DCM) for NMR experiments was purchased from Cambridge Isotope Laboratories, Inc. ^{1}H and ^{13}C NMR spectra were recorded on a 400 MHz Varian Unity Inova spectrometer, values are given in ppm, relative to the signal of residual chloroform (^{1}H: 7.26 ppm; ^{13}C: 77.16 ppm) and methylene chloride (^{1}H: 5.32; ^{13}C: 53.84). Absorption spectra were recorded on an Agilent 8453 Diode Array Spectrophotometer and on a Shimadzu Model UV-1800 spectrophotometer, fluorescence spectra on a QuantaMaster 40 spectrofluorometer (Photon Technology International, PTI) and on an Edinburgh Photonics Model FLS980 spectrofluorometer. Fluorescence lifetimes were measured on a Horiba Jobin Yvon Fluorolog 3 spectrofluorometer, samples were excited by a Jobin Yvon Model NanoLED 460 with an excitation maximum at 457 nm. Fluorescence emission for time-correlated single photon counting (TCSPC) was detected at 550 nm. BODIPY samples **B3** and **B5** failed to give reasonable results in the fluorescence lifetime experiments, because of instrumental limitations and low fluorescence quantum yield. All BODIPY−cobaloxime complexes (**1**−**5**) lacked a fluorescence signal suitable for fluorescence lifetime measurements. ATR−FT-IR (attenuated total reflectance−Fourier transform infrared) spectra were obtained on a Bruker Model Vertex 80v FT-IR spectrometer equipped with a Platinum ATR accessory. Electrochemical measurements were performed on a BioLogic Model SP-200 potentiostat/galvanostat using a glassy carbon working electrode, a platinum counter electrode, and a silver wire as the quasi-reference electrode. All measurements were carried out in degassed, dry methylene chloride with a 0.1 M tetrabutylammonium hexafluorophosphate electrolyte at a scan rate of 40 mV/s. Fc/Fc$^+$ was used as internal reference and all graphs were referenced with Fc/Fc$^+$ = 0 V. High-resolution exact mass spectrometry−electrospray ionization (HRMS-ESI) measurements were carried out on an Agilent Technologies (Santa Clara, CA) LC/MS TOF DART mass spectrometer. Samples were diluted in DCM and acetonitrile and analyzed via a 1 μL/min flow injection at 300 μL/min in a water−acetonitrile mixture 1:3 (v/v). The mass spectrometer was operated in positive-ion mode with a capillary voltage of 3.5 kV; the fragmentor and skimmer voltages were 175 and 65 V, respectively.

Crystals suitable for X-ray diffraction (XRD) were mounted on MiTeGen mounts and cooled to 110 K. X-ray intensity data were measured on a Bruker-Nonius X8 Kappa APEX II system equipped with a graphite monochromator and a Mo Kα fine-focus sealed tube (λ = 0.71073 Å). Unit-cell dimensions were determined from symmetry constrained fits of the reflections. Frames were integrated with the Bruker SAINT[45] software package using a narrow-frame algorithm. Data were corrected for absorption effects using the multiscan method (SADABS). Structures were solved using direct methods (Bruker XS)[45] and refined using the Bruker SHELX 2013[46] software package, using full-matrix least-squares refinement on F^2. All non-hydrogen atoms were identified in the original solution, or located from the difference map from refinement results. Hydrogen atoms (except for the bridging hydrogen atoms of the cobaloxime ligands) were placed at idealized positions and allowed to ride on the nearest non-hydrogen atom. Figures of the molecular structures were created using Olex^2 [47] and Mercury 3.3. Crystallographic Information Files for all structures are available in the ESI and from the Cambridge Crystallographic Data Centre (www.ccdc.cam.ac.uk).

Fluorescence quantum yields were determined by the comparative method of Williams et al.[48] Integrated fluorescence intensities of a known dye and the tested compound were compared and fluorescence quantum yields were calculated using the following equation:

$$\Phi_x = (\Phi_{st})\left(\frac{\mathrm{Grad}_x}{\mathrm{Grad}_{st}}\right)\left(\frac{\eta^2_x}{\eta^2_{st}}\right)$$

The subscripts "st" and "x" denote the standard and test, respectively, while Φ is the fluorescence quantum yield. "Grad" is the gradient obtained from the plot of integrated fluorescence intensity vs absorbance of the dye at the excitation wavelength. η represents the refractive index of the used solvents. The fluorescence quantum yield of BODIPY derivatives **B2**−**B5** was measured relative to BODIPY **B1** (Φ_F = 0.30 in DCM) at an excitation wavelength of 490 nm.[49]

Hydrogen evolution measurements were determined using the method described by Castellano and co-workers.[25] A 60% v/v acetonitrile (spectroscopic grade) solution in water was prepared and freshly distilled triethanolamine (5% v/v of the total mixture) was added. The pH was adjusted to 7.7 with 12 M HCl using a pH meter. Cobaloxime solutions of **1**−**5** (0.2 mM) were prepared in the pH-adjusted acetonitrile solutions and sonicated ca. 10 s to ensure homogeneity. These solutions were irradiated with 525 ± 10 nm (150 mW) green LED light for 17 h at 18 °C (see the electronic Supporting Information (ESI) for details). No hydrogen evolution was observed when BODIPY **B3**, **B5**, or **REF** were utilized instead of cobaloxime catalysts **1**−**5**.

Synthesis. BODIPY derivatives **B1** and **B1Me**,[50] as well as **B3** and **B3a**[44] and also BODIPY-cobaloxime complexes **1** and **1Me**,[28] were prepared following previously published procedures. Reference pyridine-cobaloxime complex **REF** (pyCo(DH)$_2$Cl) was prepared using an earlier procedure.[51]

BODIPY ***B2.*** Two hundred milligrams (200 mg, 0.616 mmol) of BODIPY **B1** was dissolved in 30 mL of DCM, and then 410 mg (1.54 mmol, 2.5 equiv) of *N*-bromosuccinimide (NBS), dissolved in 20 mL of DCM were added. After stirring for 3 h at room temperature, the organic phase was washed with 80 mL of water and 80 mL of brine and dried over Na_2SO_4. After removing the solvents, the crude was purified by column chromatography (SiO_2, DCM, 15% ethyl acetate), yielding BODIPY **B2** as a dark red solid (87%, 260 mg, 0.538 mmol). ^{1}H NMR (400 MHz, $CDCl_3$) 8.84 (dd J = 6.0 Hz, 1.6 Hz), 7.34 (dd J = 6.0 Hz, 1.6 Hz), 2.62 (s, 6H), 1.40 (s, 6H). ^{13}C NMR (400 MHz, $CDCl_3$): 155.32, 150.79, 143.48, 140.21, 137.91, 129.51, 123.37, 112.62, 14.11, 13.95. UV-vis (DCM), λ_{max} (ε [× 10^3 M^{-1} cm^{-1}]): 385

dx.doi.org/10.1021/ic500218q | Inorg. Chem. 2014, 53, 4527−4534

Scheme 2. Synthesis of BODIPY−Cobaloxime Complexes 1−5: (a) $Co(DH)(DH_2)Cl_2$, Triethylamine, Methanol; (b) *N*-Bromosuccinimide, Dichloromethane (DCM); and (c) Iodine, Iodic Acid, Ethanol

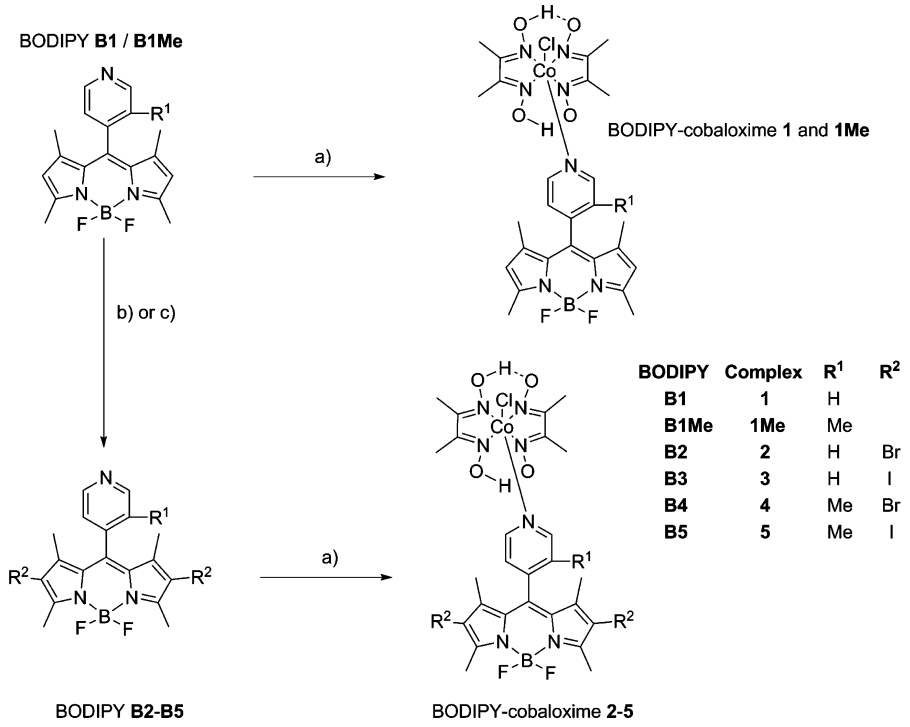

BODIPY	Complex	R^1	R^2
B1	1	H	
B1Me	1Me	Me	
B2	2	H	Br
B3	3	H	I
B4	4	Me	Br
B5	5	Me	I

(7.4), 502s (22.1), 534 (65.1) nm. Emission (DCM), λ_{Em} = 551 nm, Φ_F = 0.24, τ_F = 1.49 ns. UV-vis (acetonitrile), λ_{max} (ε [× 10^3 M^{-1} cm^{-1}]): 244 (15.2), 382 (8.8), 500s (27.4), 528 (71.5) nm. HRMS-ESI: *m*/*z*: calc'd for $C_{18}H_{16}BBr_2F_2N_3$: 483.9824 [M + H], found: 483.9825.

BODIPY−Cobaloxime 2. Here, 389.1 mg (0.933 mmol, 3 equiv) of cobaloxime $Co(DH)(DH_2)Cl_2$[51] was suspended in 20 mL of methanol and 170 μL of triethylamine was added. After the solution turned brown and cleared, 150 mg (0.311 mmol) of BODIPY **B2** in 30 mL of methanol were added and stirred for 30 min. The red microcrystalline precipitate was filtered off, washed with ice-cold methanol, and dried under vacuum, affording **2** in 90% yield (225 mg, 0.279 mmol). Recrystallization from DCM/methanol (1:3 v/v) afforded X-ray-quality crystals as dark red needles.

^{1}H NMR (400 MHz, $CDCl_3$): 8.49 (d, 2H, *J* = 6.7 Hz), 7.23 (d, 2H, *J* = 6.7 Hz), 2.59 (s, 6H), 2.44 (s, 12H), 1.14 (s, 6H). ^{13}C NMR (400 MHz, CD_2Cl_2): 156.43, 153.23, 152.66, 146.80, 139.64, 135.34, 129.24, 125.88, 113.29, 14.10, 13.84, 13.22. UV-vis (DCM), λ_{max} (ε [× 10^3 M^{-1} cm^{-1}]): 384 (10.6), 510s (28.1), 541 (73.7) nm.UV-vis (acetonitrile), λ_{max} (ε [× 10^3 M^{-1} cm^{-1}]): 247s (43.8), 382 (10.4), 505 (27.6), 533 (66.8) nm. HRMS-ESI: *m*/*z*: calc'd for $C_{26}H_{30}BBr_2ClCoF_2N_7O_4$: 807.9860 [M + H], found: 807.9846.

BODIPY B3.[44] An additional absorption spectrum was recorded in acetonitrile. UV-vis (acetonitrile), λ_{max} (ε [× 10^3 M^{-1} cm^{-1}]): 249s (17.4), 388 (11.4), 505 (28.1), 534 (70.4) nm.

BODIPY−Cobaloxime 3. Here, 117 mg (0.280 mmol, 2 equiv) of cobaloxime $Co(DH)(DH_2)Cl_2$[51] was suspended in 15 mL of methanol and 51 μL of triethylamine was added. After the solution turned brown and cleared, 81 mg (0.140 mmol) of BODIPY **B3** in 15 mL methanol/15 mL DCM were added and stirred for 15 min, while cooling with ice. The dark red microcrystalline precipitate was filtered off, washed with some ice-cold methanol, and dried under vacuo, affording **3** in 97% yield (123 mg, 0.136 mmol). Recrystallization from DCM/diethyl ether (1:3 v/v) afforded X-ray quality crystals as dark red needles.

^{1}H HMR (400 MHz, $CDCl_3$): 8.49 (d, 2H, *J* = 4.5 Hz), 7.22 (d, 2H, *J* = 4.8 Hz), 2.63 (s, 6H), 2.44 (s, 12H), 1.15 (s, 6H). ^{13}C NMR (400 MHz, CD_2Cl_2): 159.11, 153.15, 152.57, 147.11, 146.05, 144.31, 134.44, 129.97, 125.82, 17.12, 16.44, 13.21. UV-vis (DCM), λ_{max} (ε [× 10^3 M^{-1} cm^{-1}]): 392 (9.5), 517s (25.9), 549 (69.1) nm. UV-vis (acetonitrile), λ_{max} (ε [× 10^3 M^{-1} cm^{-1}]) 253s (38.5), 392 (11.5), 509 (27.3), 541 (67.7) nm. HRMS-ESI: *m*/*z*: calc'd for $C_{26}H_{30}BClCoF_2I_2N_7O_4$: 901.9602 [M + H], found: 901.9617.

BODIPY derivatives **B4** and **B5** were prepared following similar procedures as other BODIPY derivatives **B2** or **B3**, respectively, starting from BODIPY **B1Me**.[50] The corresponding BODIPY−cobaloxime complexes **4** and **5** were prepared in a similar way as BODIPY−cobaloxime complexes **2** and **3**.

BODIPY B4. **B4** was prepared from 80 mg (0.23 mmol) of **B1Me**. Yield: 88% (102 mg, 0.205 mmol). ^{1}H NMR (400 MHz, $CDCl_3$): 8.67 (dd, 2H, *J* = 6.0 Hz), 7.24 (s, 1H), 2.62 (s, 6H), 2.26 (s, 3H), 1.38 (s, 6H). ^{13}C NMR (400 MHz, CD_2Cl_2): 155.14, 152.31, 148.92, 142.44, 140.33, 138.34, 131.32, 129.23, 122.83, 112.39, 16.24, 13.98, 13.51. UV-vis (DCM), λ_{max} (ε [× 10^3 M^{-1} cm^{-1}]): 383 (5.9), 507s (20.0), 533 (55.9) nm. Emission (DCM): λ_{Em} 549 nm, Φ_F 0.25, τ_F = 3.92 ns. UV-vis (acetonitrile), λ_{max} (ε [× 10^3 M^{-1} cm^{-1}]): 382 (7.4), 503s (27.4), 527 (69.6) nm. HRMS-ESI: *m*/*z*: calc'd for $C_{19}H_{18}BBr_2F_2N_3$: 497.9968 [M + H], found: 497.9988.

BODIPY−Cobaloxime 4. BODIPY−cobaloxime **4** was prepared from 63 mg (0.13 mmol) of **B4**. Yield: 97% (103 mg/0.137 mmol). ^{1}H NMR (400 MHz, $CDCl_3$): 8.33 (d, 1H, *J* = 9 Hz), 8.29 (s, 1H), 7.08 (d, 1H, 6 Hz), 2.63 (s, 6H), 2.44 (s, 12H), 2.15 (s, 3H), 1.13 (s, 6H). ^{13}C NMR (400 MHz, CD_2Cl_2): 156.33, 153.05, 152.77, 150.23, 146.29, 139.09, 134.82, 128.43, 125.18, 113.10, 16.90, 14.08, 13.21, 13.11. UV-vis (DCM), λ_{max} (ε [× 10^3 M^{-1} cm^{-1}]): 383 (8.7), 511s (25.5), 540 (68.9) nm. UV-vis (acetonitrile), λ_{max} (ε [× 10^3 M^{-1} cm^{-1}]): 380 (11.0), 505s (31.1), 532 (76.1) nm. HRMS-ESI: *m*/*z*: calc'd for $C_{27}H_{32}BBr_2ClCoF_2N_7O_4$: 819.9959 [M+], found: 819.9952.

BODIPY B5. **B5** was prepared from 80 mg (0.23 mmol) of **B1Me**. Yield: 83% (116 mg/0.196 mmol). ^{1}H NMR (400 MHz, $CDCl_3$): 8.67 (dd, 2H, *J* = 5.7 Hz), 7.23 (s, 1H), 2.66 (s, 6H), 2.25 (s, 3H), 1.40 (s, 6H). ^{13}C NMR (400 MHz, CD_2Cl_2): 58.00, 152.48, 149.07, 145.16, 142.81, 137.71, 131.37, 130.19, 122.90, 86.32, 16.83, 16.38, 16.28. UV-vis (DCM), λ_{max} (ε [× 10^3 M^{-1} cm^{-1}]): 390 (7.4), 514s (24.3), 539 (64.3) nm. Emission (DCM): λ_{Em} 559 nm, Φ_F 0.02. UV-vis (acetonitrile), λ_{max} (ε [× 10^3 M^{-1} cm^{-1}]): 391 (6.8), 508s (24.1), 534 (60.2) nm. HRMS-ESI: *m*/*z*: calc'd for $C_{19}H_{18}BF_2I_2N_3$: 591.9978 [M + H], found: 591.9736.

dx.doi.org/10.1021/ic500218q | *Inorg. Chem.* 2014, 53, 4527−4534

BODIPY–Cobaloxime **5**. BODIPY–cobaloxime **5** was prepared from 45 mg (0.07 mmol) of **B5**. Yield: 96% (68 mg/0.080 mmol). ^{1}H NMR (400 MHz, CD_2Cl_2) 8.28 (d, 1H, J = 3.0 Hz), 8.25 (s, 1H), 7.14 (d, 1H, J = 6.0 Hz), 2.56 (s, 6H), 2.40 (s, 12H), 2.14 (s, 3H), 1.13 (s, 6H).

^{13}C NMR (400 MHz, CD_2Cl_2): 156.44, 153.07, 152.89, 150.28, 146.36, 139.14, 134.88, 128.52, 125.24, 113.18, 16.91, 14.12, 13.21, 13.14. UV-vis (DCM), λ_{max} (ε [× 10^3 M^{-1} cm^{-1}]): 392 (12.7), 519s (27.4), 548 (60.0) nm. UV-vis (acetonitrile), λ_{max} (ε [× 10^3 M^{-1}, cm^{-1}]): 384 (8.7), 511s (25.6), 540 (68.9) nm. HRMS-ESI: m/z: calc'd for $C_{27}H_{32}BClCoF_2I_2N_7O_4$: 915.5969 [M], found: 915.9768.

RESULTS AND DISCUSSION

Synthetic Aspects. The parent, unsubstituted pyridyl-BODIPY **B1** was prepared as previously reported;[49] in addition, it is the starting material for 2,6-dibromo-substituted BODIPY **B2** as well as for the previously reported 2,6-diiodo derivative **B3**[44] (see Scheme 2). Bromination of BODIPY **B1** leads to the 2,6-dibromo-substituted BODIPY **B2**, which was accomplished using *N*-bromosuccinimide (NBS) in dichloromethane (DCM). The synthesis and characterization of BODIPY–cobaloxime complex **1**, based on BODIPY **B1**, without halogen substituents in the 2- and 6-positions of the BODIPY core, was reported earlier.[28] Based on this procedure, these BODIPY–cobaloxime complexes were synthesized starting from the cobaloxime precursor $Co^{III}(DH)(DH_2)Cl_2$, which was prepared following standard protocol.[51] Following macrocyclization, addition of the BODIPY derivatives **B2** or **B3** in methanol leads to BODIPY–cobaloxime complexes **2** and **3**, which precipitate readily from solution and are directly obtained in high purity and yield without further purification. *Meso*-methylpyridine BODIPY–cobaloxime complexes **4** and **5** are synthesized from the dihalogenated derivatives of a previously reported *meso*-methylpyridine BODIPY (**B1Me**).[50] Halogenation and cobaloxime complex formation was accomplished following similar procedures to the aforementioned BODIPY–cobaloxime complexes **2** and **3** in excellent yields. All newly prepared BODIPY–cobaloxime complexes are consistent with our earlier results that *meso*-pyridyl BODIPY and *meso*-methylpyridyl BODIPY derivatives readily form stable complexes with cobaloxime.[28]

Crystallographic Analysis. The molecular structures of BODIPY–cobaloxime complexes **2** and **3** are shown in Figure 1, and these are compared to the crystal structure of **1**.[28] Important crystallographic information is summarized in Table 1 and with further details in Table S1 in the ESI. X-ray-quality crystals of **2** and **3** were obtained by recrystallization from DCM/methanol 1:3 (v/v) (complex **2**) or DCM/diethyl ether 1:3 (v/v) (complex **3**). The molecular structure of BODIPY–cobaloxime **2** contains one molecule of co-crystallized DCM per complex molecule (see Figure 2). Replacement of methanol with diethyl ether was necessary to afford X-ray-quality crystals for BODIPY–cobaloxime complex **3**. As shown in our earlier report,[28] we found that the methyl group on the pyridyl linker leads to major disorder in the crystal structure, which most likely prevented us from obtaining X-ray-quality crystals for complexes **4** and **5**.

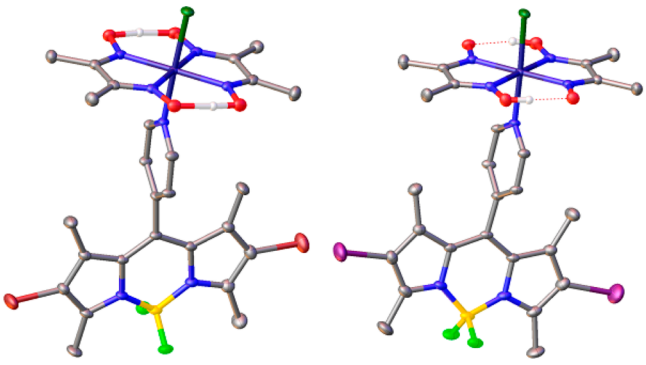

Figure 1. Molecular structure of BODIPY–cobaloxime complexes **2** (left) and **3** (right). ORTEP ellipsoids represent 50% probability. Hydrogen atoms (except bridging atoms of the cobaloxime macrocycle) and solvent molecules are omitted for clarity.

Table 1. Sample and Crystal Data: Selected Details about Data Collection and Crystal Refinement for BODIPY–Cobaloxime Complexes 2 and 3

	2	3
CCDC reference number	982 729	982 728
chemical formula	$C_{27}H_{32}BBr_2Cl_3CoF_2N_7O_4$	$C_{28.50}H_{36}BCl_2CoF_2I_2N_7O_{4.50}$
formula weight	892.50	981.08
temperature	110(2) K	110(2) K
wavelength	0.71073 Å	0.71073 Å
crystal size	0.040 mm × 0.070 mm × 0.280 mm	0.040 mm × 0.140 mm × 0.280 mm
crystal habit	red plate	intense red plate
crystal system	triclinic	triclinic
space group	$P\bar{1}$	$P\bar{1}$
unit-cell dimensions	a = 8.6485(4) Å	a = 8.6647(4) Å
	b = 12.5074(5) Å	b = 13.9199(5) Å
	c = 16.9781(8) Å	c = 16.0550(6) Å
	α = 82.983(2)°	α = 101.352(2)°
	β = 79.078(2)°	β = 102.329(2)°
	γ = 72.351(2)°	γ = 95.691(2)°
volume	1714.27(13) Å^3	1834.49(13) Å^3
Z	2	2
density (calculated)	1.729 g/cm^3	1.776 g/cm^3
absorption coefficient	3.121 mm^{-1}	2.352 mm^{-1}
F(000)	892	964
theta range for data collection	1.71°–30.71°	1.77°–30.79°
reflections collected	46 982	54 448
independent reflections	10617 [R(int) = 0.0352]	11375 [R(int) = 0.0360]
coverage of independent reflections	99.6%	99.0%
goodness-of-fit on F^2	1.018	1.035
final R indices	8183 data; $I > 2\sigma(I)$: $R1$ = 0.0365, $wR2$ = 0.0882	8838 data; $I > 2\sigma(I)$: $R1$ = 0.0421, $wR2$ = 0.1003
	all data: $R1$ = 0.0557, $wR2$ = 0.0958	all data: $R1$ = 0.0600, $wR2$ = 0.1089
largest diff. peak and hole	0.815 and −0.923 e Å^{-3}	3.555 and −1.213 e Å^{-3}

Differences between the molecular structures of **1**, **2**, and **3** include the absence of a solvent molecule in the molecular structure of complex **1**. In addition, while complex **1** crystallizes

dx.doi.org/10.1021/ic500218q | Inorg. Chem. 2014, 53, 4527–4534

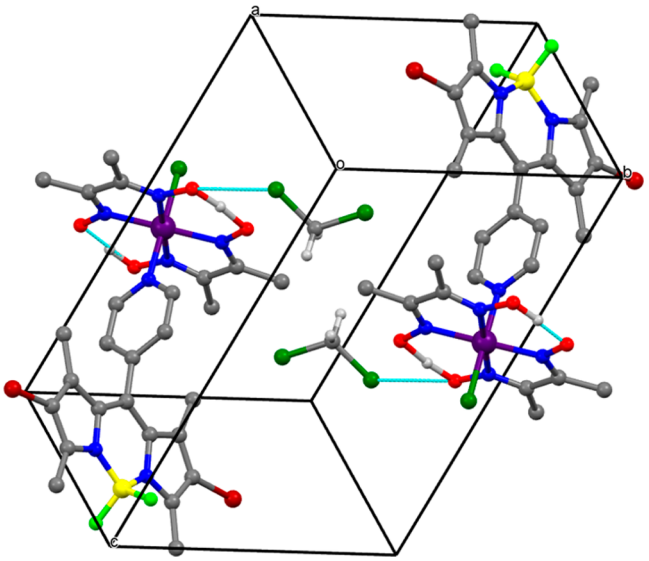

Figure 2. Molecular structure (unit cell) of BODIPY–cobaloxime complex **2**, illustrating the complex–solvent (CH_2Cl_2) interactions and the highly ordered structure. Hydrogen atoms (except bridging atoms of the cobaloxime macrocycle and in the solvent molecules) are omitted for clarity.

in the monoclinic system $P2_1/c$, complexes **2** and **3** crystallize in the triclinic system $P\bar{1}$. No significant changes of bond lengths and angles between complexes **1**, **2**, and **3** could be identified (see Table S2 in the ESI). Based on these results, we can conclude that bromo- or iodo- substitution on the BODIPY center does not lead to significant changes in the molecular structure of the presented BODIPY–cobaloxime complexes.

Spectroscopic Properties. The absorption and fluorescence features of the novel BODIPY–cobaloxime complexes **2**–**5** and their parent BODIPY derivatives **B2**–**B5** show similar trends to their previously described, nonhalogenated analogues[28] (see Table 2 for details, as well as Figure 3 and Figure S4 in the Supporting Information). Following complexation, the main absorption band of BODIPY derivatives **B2**–**B5** undergoes a bathochromic shift between 5 and 9 nm. In acetonitrile, compared to DCM, all absorption features appear hypsochromically shifted (5–6 nm for BODIPY **B2**–**B5** and 8 nm for BODIPY–cobaloxime complexes **2**–**5**). The methyl substituent on the pyridine linker did not significantly influence the absorption properties. Iodization of the BODIPY core, compared to bromination, leads to a slightly larger bathochromic shift of the main absorption band of the BODIPY (~2 nm) upon complexation with cobaloxime.

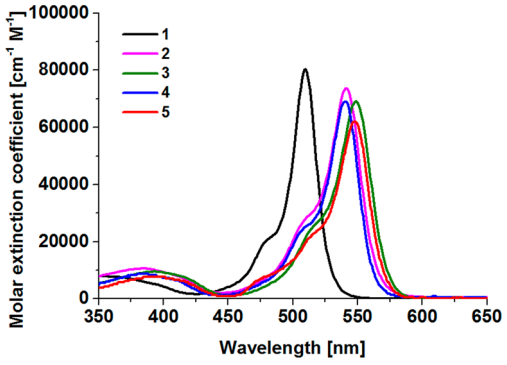

Figure 3. Molar extinction coefficients of BODIPY–cobaloxime complexes **1**–**5** in dichloromethane (DCM). Data of **1** derived from ref 28.

The halogenation of the BODIPY core by either bromine or iodine leads to a quenched fluorescence due to the heavy atom effect, presumably by formation of the photoexcited triplet state, as described earlier.[29,41,42] However, while the fluorescence quantum yields in DCM of brominated BODIPY derivatives **B2** and **B4** are still 0.24 and 0.25, respectively, iodated derivatives **B3** and **B5** show a low fluorescence quantum yield of 0.03 and 0.02, respectively. Upon complexation with cobaloxime, the remaining BODIPY centered fluorescence emission is quantitatively quenched in all complexes. This could be due to electron transfer from the photoexcited BODIPY to the cobaloxime and/or additional radiationless deactivation of the photoexcited states. Given that electron transfer is essential for the observed photocatalytic hydrogen generation,[10,14,37–39] it is likely that electron transfer from the photoexcited BODIPY to the cobaloxime catalyst occurs, since we observe photocatalytic hydrogen evolution for these complexes.[4,15,16,22]

Electrochemical Characterization. The effects of halogenation on the electrochemical properties of the BODIPY chromophores are significant. Halogenation of the BODIPY molecule leads to shifts of both reduction and oxidation potentials to more-positive values, which is consistent with previously reported results[40] (see Table 3). The assignment and discussion of the individual redox processes for this class of molecules has been previously reported.[28] The identity of the halogen substituent (i.e., bromine or iodine) did not produce

Table 2. Photophysical Data of BODIPY Derivatives B1–B5 and BODIPY–Cobaloxime Complexes 1-5 in Dichloromethane (DCM) and Acetonitrile (MeCN)

	DCM				MeCN				
	λ_{Abs} (nm)	ε ($\times 10^3$ cm^{-1} M^{-1})	λ_{Em} (nm)	Φ_F	λ_{Abs} (nm)	ε ($\times 10^3$ cm^{-1} M^{-1})	λ_{Em} (nm)	Φ_F	TON molar equiv. H_2
1	509[a]	80.3[a]	n.a.[b]		504	69.0	n.a.[b]		0
B2	534	65.1	551	0.24	528	71.5	545	0.16	
2	541	73.7	n.a.[b]		533	66.8	n.a.[b]		9.3
B3	540[c]	78.8[c]	559	0.03	534	70.4	555	0.02	
3	549	69.1	n.a.[b]		541	67.7	n.a.[b]		10.1
B4	533	55.9	549	0.25	527	69.6	549	0.18	
4	540	68.9	n.a.[b]		532	76.1	n.a.[b]		19.1
B5	539	64.3	559	0.02	534	60.2	555	0.01	
5	548	66.0	n.a.[b]		540	69.1	n.a.[b]		30.9

[a]Data taken from ref 28. [b]Not applicable; no notable fluorescence signal could be detected. [c]Data taken from ref 44.

dx.doi.org/10.1021/ic500218q | Inorg. Chem. 2014, 53, 4527–4534

Table 3. Electrochemical Data for BODIPY Derivatives B1−B5 and BODIPY−Cobaloxime Complexes 1−5 in Degassed Dichloromethane (DCM)

	Reduction Potential (V)[a]			Oxidation Potential (V)[a]		
	Red3	Red2	Red1[b]	Ox1[b]	Ox2	Ox3
B1		−1.60			0.72[c]	0.88[c]
1[d]	−1.58	−1.48	−0.83	0.81	0.86[c]	
B2		−1.37			0.86[c]	1.04[c]
2	−1.59[c]	−1.30[c]	−0.74	0.80	1.01[c]	
B3		−1.38			0.85[c]	1.02[c]
3	−1.60[c]	−1.35[c]	−0.76	0.79	0.96[c]	
B4		−1.37			0.93[c]	1.07[c]
4	−1.60[c]	−1.31[c]	−0.73	0.79	0.99[c]	
B5		−1.38			0.96[c]	1.09[c]
5	−1.61[c]	−1.34[c]	−0.73	0.79	1.01[c]	
REF[d,e]		−1.51	−0.96	0.74		

[a]All values given in V, relative to Fc/Fc^+ = 0 V. [b]Cobaloxime centered potentials, not applicable for BODIPY molecules. [c]Irreversible wave. Please note that the oxidation and reduction potentials (except Red1 and Ox1) cannot be definitively assigned due to overlapping potentials of the BODIPY and cobaloxime components. [d]Values taken from ref 28. [e]Reference pyridine−cobaloxime complex: $pyCo(DH)_2Cl$.[51]

notable differences for the BODIPY oxidation and reduction potentials. Complexation of BODIPY derivatives **B2**−**B5** with cobaloxime leads to similar observations described for other BODIPY−cobaloxime complexes: the redox potentials shift to more-positive values.[28] The catalytically relevant Co^{III}/Co^{II} redox couple is of special interest for hydrogen production, and can be assigned by comparison with the reference pyridine−cobaloxime complex **REF** ($pyCo(DH)_2Cl$)[51] (−0.96 V in DCM, with Fc/Fc^+ = 0 V). In the nonhalogenated BODIPY−cobaloxime complex **1**, the Co^{III}/Co^{II} redox couple is significantly reduced, by 0.13 V.[28] For the halogenated complexes **2**−**5**, the potential of the Co^{III}/Co^{II} redox couple is further reduced, by 0.22 V (complex **2**), 0.20 V (complex **3**), and 0.23 V (complexes **4** and **5**), when compared to complex **REF**. This further reduction in the potential of the Co^{III}/Co^{II} redox couple, compared to our earlier reports,[28] is a promising step toward the optimization of BODIPY−cobaloxime complexes for photocatalytic hydrogen generation. Unfortunately, overlap of other BODIPY and cobaloxime redox potentials, for oxidation as well as for reduction, makes it impossible to definitively assign the other observed waves to specific redox processes.

Photocatalytic Hydrogen Evolution. Catalytic hydrogen evolution was observed when BODIPY−cobaloxime complexes **2**−**5** are used as photocatalysts. Compounds **2**, **3**, **4**, and **5** exhibited turnover numbers (TONs) of 9.3, 10.1, 19.1, and 30.9 equiv. of hydrogen per catalyst, respectively, after 17 h of illumination with a λ = 525 ± 10 nm LED operating at 150 mW. The hydrogen evolution profiles for these complexes and the instantaneous hydrogen formation rates are shown in Figures 4 and 5, respectively.

Halogenation of the BODIPY chromophore is required for catalytic proton reduction in our system; BODIPY−cobaloxime complexes **1** and **1Me** show no production of hydrogen outside of experimental error. Previous studies have suggested that the population of the photoexcited triplet state in the chromophore is important for photocatalytic hydrogen production with cobaloxime catalysts.[15,16] Our results support this finding and suggests that only the triplet state of the BODIPY

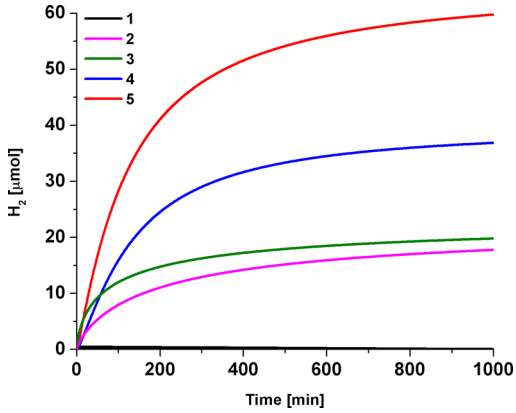

Figure 4. Hydrogen evolution profiles of BODIPY−cobaloxime complexes irradiated at 525 nm (150 mW) at pH 7.7 in 6:4 acetonitrile/water solution with 5% triethanolamine as an electron donor. Compounds **1** and **1Me** showed negligible activity.

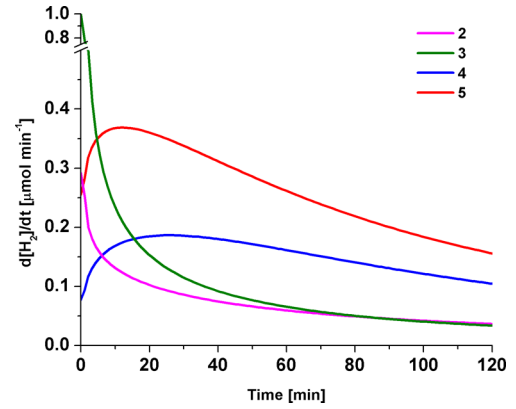

Figure 5. Plots of instantaneous molar hydrogen turnover frequency for the first 2 h of irradiation of systems containing cobaloxime catalysts **2** (magenta), **3** (olive), **4** (blue), and **5** (red). Derived from data in Figure 4.

chromophores is capable of efficiently transferring an electron to the cobaloxime catalytic center. A mechanism proposed earlier for comparable BODIPY photosensitizers is most likely to happen in the present case.[43] We further observe a faster peak instantaneous catalytic activity in molecules that contain iodine versus those that contain bromine (recall Figure 5). This is consistent with the iodized photosensitizers having a faster rate for singlet−triplet intersystem crossing, presumably due to the larger heavy atom effect of iodine versus bromine,[29,41,42] and is further supported by the fluorescence data in Table 2. The fluorescence of the iodinated BODIPY compounds **B3** and **B5** is nearly fully quenched, while the brominated BODIPY compounds **B2** and **B4** retain significant fluorescence. Therefore, we propose that the relatively faster instantaneous rate of hydrogen production of the iodinated derivatives **3** and **5**, when compared to the brominated derivatives **2** and **4**, is due to their ability to form the triplet excited state more efficiently and quickly. This is then able to transfer an electron to the cobaloxime to continue the catalytic cycle.

Methylation of the pyridyl linker (complexes **4** and **5**) results in a marked increase in the proton reduction turnover number (TON), relative to the unfunctionalized analogues **2** and **3**. In previous studies,[50] we demonstrated that the pyridyl nitrogen atom is more basic in BODIPY **B1Me** than in **B1**. More

dx.doi.org/10.1021/ic500218q | Inorg. Chem. 2014, 53, 4527−4534

generally, we found that the pyridyl nitrogen becomes more basic with increasingly electron-donating substituents. As we have previously observed, increasing the basicity of the pyridyl linkage improves the stability of the BODIPY−cobaloxime complex.[28] We conclude that the increased TON in the methyl-substituted complexes **4** and **5**, relative to **2** and **3**, is a result of greater stability of the complex. Computing the derivative of the hydrogen evolution profiles (Figure 5), with respect to time, lends insight into whether the particular catalyst modifications lead to TON variations due to improved photon-to-hydrogen efficiency or changes in catalyst stability. Since the photon flux is constant under our experimental conditions, faster rates of H_2 production necessarily have higher quantum efficiencies.

Upon illumination, complexes **2** and **3** have initially fast rates of hydrogen production with no observed induction period, with initial rates of 0.29 and 1.00 μmol min^{-1}. These rates are 4.0 and 4.2 times higher than the peak turnover frequency of their methylated counterparts **4** and **5**. The peak hydrogen production rate for **4** and **5** (0.19 and 0.37 μmol min^{-1}) occurs after a measurable induction period of 12 and 21 min, respectively. A similar induction period has been previously observed in studies of platinum-sensitized cobaloximes,[14] with the reduction of Co^{III} to Co^{II} being suggested as a required precatalytic step.[13] The BODIPY complexes with unsubstituted pyridyl linkers (**2** and **3**) have a faster initial rate of photocatalysis, and thus have higher initial quantum efficiencies for electron transfer between the BODIPY chromophores and the cobaloxime catalytic center. However, as shown in Figure 5, **2** and **3** quickly become catalytically inactive, whereas **4** and **5** remain stable for significantly longer. This difference in catalyst lifetime can be explained by the aforementioned higher stability of the complexes **4** and **5**, and this increased catalyst lifetime explains the increased TON observed for the systems that contain a stronger dative interaction between the cobaloxime and BODIPY.

To explain the relatively faster initial rate for hydrogen production in **2** and **3**, we turn to the structural parameters of our previously reported cobaloxime−BODIPY compounds.[28] We found that BODIPYs that have a substituent in the *meta* position of the pyridine force the pyridyl group into a more perpendicular torsion angle between the pyridyl and BODIPY core than in unsubstituted BODIPY complexes,[28] and we expect this geometric trend to hold for cobaloxime complexes **2**−**5**. Studies by Wenger and co-workers on electron transfer through oligophenylene bridges have shown that π-systems bridged by groups that introduce torsion between phenyl units lowers the electronic coupling between donors and acceptors.[52] We feel that a similar effect is operating here, where the presence of a methyl group decreases the electronic coupling between the BODIPY and cobaloxime versus the unsubstituted pyridyl linker. This decrease reduces the overall rate of excited-state electron transfer and ultimately reduces the initial quantum yield for hydrogen production in **4** and **5** vs **2** and **3** under these conditions.

We investigated the possibility of bimolecular hydrogen production through dissociated cobaloxime and BODIPY photosensitizer by combining equimolar amounts of the reference cobaloxime **REF** (py$Co(DH)_2Cl$) and the previously reported *meso*-pyridyl *N*-methylated derivative of BODIPY **B3**: **B3a**.[44] Methylation of the BODIPYs pyridyl nitrogen atom ensures that the chromophore is unable to coordinate to the Co metal center in situ, while maintaining largely similar ground state redox potentials as **B3**. In addition, a highly populated triplet state was reported previously for **B3a**.[44] Hydrogen production from the bimolecular system **REF**/**B3a** is substoichiometric (ca. 0.6 turnovers), and the peak rate of hydrogen production is ∼40 times smaller than that of cobaloxime complex **3** (where **B3** and the cobaloxime catalyst are covalently linked). A plot of the hydrogen evolution profile of the bimolecular system and its derivative curve can be found in the ESI (Figure S1). This comparatively low activity indicates that covalent attachment of the BODIPY to the cobaloxime is required for catalysis in this system, evidence that refutes recent computational studies[36] suggesting inherent photoinstability for such linkages.

CONCLUSION

Four novel hydrogen evolving photocatalytic complexes are synthesized and characterized. We were able to demonstrate catalytic light-driven hydrogen evolution for halogenated BODIPY−cobaloxime complexes **2**−**5**. Key for the preparation of these effective photocatalysts was the halogenation of the BODIPY chromophores with either bromine or iodine. From this, we conclude that the photoexcited triplet state is necessary for efficient electron transfer between the BODIPY chromophore and the attached cobaloxime catalyst. This is supported by earlier studies where the triplet state was necessary for catalytic hydrogen production.[15,17,43] Catalytic activity, as measured by the turnover number (TON), was further enhanced with an electron-donating methyl substituent on the chromophore-catalyst pyridyl linker. We attribute this improvement to improved stability of the photocatalytic system due to the increased basicity of the pyridyl nitrogen.[50] However, improvements in stability and TON for the methyl-substituted linkers are tempered by lower initial hydrogen formation rates, relative to the unsubstituted pyridyl linkers. This interplay between catalyst stability and electron transfer efficiency is an important design consideration for covalently linked chromophore-catalyst systems. BODIPY-cobaloxime molecular complexes are promising proton reduction photocatalysts and demonstrate that accessing triplet states and improving linker stability is essential for increasing the photocatalytic TON.

ASSOCIATED CONTENT

Supporting Information

Details for photocatalytic hydrogen generation and reference measurements. Crystallographic tables and procedures, numbered molecular structures. Additional absorption spectra of complexes **1**−**5** in acetonitrile. Cyclic voltammograms, solid-state ATR−FT-IR and ^1H and ^{13}C NMR spectra, and representative mass spectra of new compounds. CCDC Nos. 982729 (**2**) and 982729 (**3**). Tables. This material is available free of charge via the Internet at http://pubs.acs.org.

AUTHOR INFORMATION

Corresponding Author

*Email: wwweare@ncsu.edu.

Notes

The authors declare no competing financial interest.

ACKNOWLEDGMENTS

This work was supported by startup funding from North Carolina State University. We thank Dr. George Dubay

(Department of Chemistry, Duke University) for obtaining the mass spectra. We are grateful to Dr. Rony S. Khnayser, Dr. Jonathan Lindsey, and Dr. Ana Soares (Department of Chemistry, NCSU) for assistance with instrumentation and helpful discussion and Dr. Achmed El-Shafei and Hammad Cheema (College of Textiles, NCSU) for additional instrumental support.

REFERENCES

(1) Faunce, T. A.; Lubitz, W.; Rutherford, A. W.; MacFarlane, D.; Moore, G. F.; Yang, P.; Nocera, D. G.; Moore, T. A.; Gregory, D. H.; Fukuzumi, S.; Yoon, K. B.; Armstrong, F. A.; Wasielewski, M. R.; Styring, S. *Energy Environ. Sci.* **2013**, *6*, 695.
(2) Styring, S. *Faraday Discuss.* **2012**, *155*, 357.
(3) Tchibana, Y.; Vaysierres, L.; Durrant, J. R. *Nat. Photonics* **2012**, *6*, 511.
(4) Artero, A.; Chavarot-Kerlidou, M.; Fontecave, M. *Angew. Chem., Int. Ed.* **2011**, *50*, 7238.
(5) Du, P.; Eisenberg, R. *Energy Environ. Sci.* **2012**, *5*, 6012.
(6) Kanan, M. W.; Nocera, D. G. *Science* **2006**, *321*, 1072.
(7) Jiao, F.; Frei, H. *Angew. Chem., Int. Ed.* **2009**, *48*, 1841.
(8) Wang, C.; deKrafft, K. E.; Lin, W. *J. Am. Chem. Soc.* **2012**, *134*, 7211.
(9) Ozawa, H.; Sakai, K. *Chem. Commun.* **2011**, *47*, 2227.
(10) Dempsey, J. L.; Brunschwig, B. S.; Winkler, J. R.; Gray, H. B. *Acc. Chem. Res.* **2009**, *42*, 1995.
(11) Wang, M.; Sun, L. *ChemSusChem* **2010**, *3*, 551.
(12) Hawecker, J.; Lehn, J.-M.; Ziessel, R. *Nouv. J. Chim.* **1983**, *7*, 271.
(13) Du, P.; Knowles, K.; Eisenberg, R. *J. Am. Chem. Soc.* **2008**, *130*, 12576.
(14) Du, P.; Schneider, J.; Luo, G.; Brennessel, W. W.; Eisenberg, R. *Inorg. Chem.* **2009**, *48*, 4952.
(15) Lazarides, T.; McCormick, T.; Du, P.; Luo, G.; Lindley, B.; Eisenberg, R. *J. Am. Chem. Soc.* **2009**, *131*, 9192.
(16) McCormick, T. M.; Calitree, B. D.; Orchard, A.; Kraut, N. D.; Bright, F. V.; Detty, M. R.; Eisenberg, R. *J. Am. Chem. Soc.* **2010**, *132*, 15480.
(17) McCormick, T. M.; Han, Z.; Weinberg, D. J.; Brennessel, W. W.; Holland, P. L.; Eisenberg, R. *Inorg. Chem.* **2011**, *50*, 10660.
(18) Veldkamp, B. S.; Han, W.-S.; Dyar, S. M.; Eaton, S. W.; Ratner, M. A.; Wasielewski, M. R. *Energy Environ. Sci.* **2013**, *6*, 1917.
(19) Zhang, P.; Wang, M.; Li, C.; Li, X.; Dong, J.; Sun, L. *Chem. Commun.* **2010**, *46*, 8806.
(20) Peuntinger, K.; Lazarides, T.; Dafnomili, D.; Charalambidis, G.; Landrou, G.; Kahnt, A.; Sabatini, R. P.; McCamant, D. W.; Gryko, D. T.; Coutsolelos, A. G.; Guldi, D. M. *J. Phys. Chem. C* **2013**, *117*, 1647.
(21) Natali, M.; Argazzi, R.; Chiorboli, C.; Iengo, E.; Scandola, F. *Chem.—Eur. J.* **2013**, *19*, 9261.
(22) Lazarides, T.; Delor, M.; Sazanovich, I. V.; McCormick, T. M.; Georgakaki, I.; Charalambidis, G.; Weinstein, J. A.; Coutsolelos, A. G. *Chem. Commun.* **2014**, *15*, 521.
(23) Natali, M.; Orlandi, M.; Chiorboli, C.; Iengo, E.; Bertolasi, V.; Scandola, F. *Photochem. Photobiol. Sci.* **2013**, *12*, 1749.
(24) Lazarides, T.; Delor, M.; Sazanovich, I. V.; McCormick, T. M.; Georgakaki, I.; Charalambidis, G.; Weinstein, J. A.; Coutsolelos, A. G. *Chem. Commun.* **2014**, *50*, 521−523.
(25) Khnayzer, R. S.; McCusker, C. E.; Olaiya, B. S.; Castellano, F. N. *J. Am. Chem. Soc.* **2013**, *135*, 14068.
(26) Lakadamyali, F.; Reisner, E. *Chem. Commun.* **2011**, *47*, 1695.
(27) Andreiadis, E. S.; Jacques, P.-A.; Tran, P. D.; Lyris, A.; Chavarot-Kerlidou, M.; Jousselme, B.; Metheron, M.; Pécault, J.; Palacin, S.; Fontecave, M.; Artero, V. *Nat. Chem.* **2013**, *5*, 48.
(28) Bartelmess, J.; Weare, W. W.; Sommer, R. D. *Dalton Trans.* **2013**, *42*, 14883.
(29) Loudet, A.; Burgess, K. *Chem. Rev.* **2007**, *107*, 4891.
(30) Ulrich, G.; Ziessel, R.; Harriman, A. *Angew. Chem., Int. Ed.* **2008**, *47*, 1184.
(31) Lim, S. H.; Thivierge, C.; Nowak-Sliwinska, P.; Han, J.; van den Bergh, H.; Wagnières, G.; Burgess, K.; Lee, H. B. *J. Med. Chem.* **2010**, *53*, 2865.
(32) Nepomnyashchii, A. B.; Lippard, J. L. *Acc. Chem. Res.* **2012**, *45*, 1844.
(33) El-Khouly, M. E.; Fukuzumi, S.; D'Souza, F. *ChemPhysChem* **2014**, *15*, 30.
(34) Zhao, J.; Wu, W.; Sun, J.; Guo, S. *Chem. Soc. Rev.* **2013**, *42*, 5323.
(35) Khan, T. K.; Bröring, M.; Mathur, S.; Ravikanth, M. *Coord. Chem. Rev.* **2013**, *257*, 2348.
(36) Manton, J. C.; Long, C.; Vos, J. G.; Pryce, M. T. *Phys. Chem. Chem. Phys.* **2014**, *16*, 5229−5236.
(37) Razavet, M.; Artero, V.; Fontecave, M. *Inorg. Chem.* **2005**, *44*, 4786.
(38) Baffert, C.; Artero, V.; Fontecave, M. *Inorg. Chem.* **2007**, *46*, 1817.
(39) Solis, B. H.; Hammes-Schiffer, S. *J. Am. Chem. Soc.* **2011**, *133*, 19036.
(40) Krumova, K.; Cosa, G. *J. Am. Chem. Soc.* **2010**, *132*, 17560.
(41) Atilgan, S.; Ekmekci, Z.; Dogan, A. L.; Guc, D.; Akkaya, E. U. *Chem. Commun.* **2006**, 4398.
(42) Kamkaew, A.; Sim, S. H.; Lee, H. B.; Kiew, L. V.; Chung, L. Y.; Burgess, K. *Chem. Soc. Rev.* **2013**, *42*, 77.
(43) Sabatini, R. B.; McCormick, T. M.; Lazarides, T.; Wilson, K. C.; Eisenberg, R.; McCamant, D. W. *J. Phys. Chem. Lett.* **2011**, *2*, 223.
(44) Caruso, E.; Banfi, S.; Barbieri, P.; Leva, B.; Orlandi, V. T. *J. Photochem. Photobiol., B* **2012**, *114*, 44.
(45) Bruker-Nonius. *SAINT, SADABS*; Bruker AXS, Inc.: Madison, WI, USA, 2009.
(46) Sheldrick, G. M. *Acta Crystallogr., Sect A: Found. Crystallogr.* **2008**, *A64*, 112.
(47) Dolomanov, O. V.; Bourhis, L. J.; Gildea, R. J.; Howard, J. A. K.; Puschmann, J. A. K. *J. Appl. Crystallogr.* **2009**, *42*, 339.
(48) Williams, A. T. R.; Winfield, S. A.; Miller, J. N. *Analyst* **1983**, *108*, 1067.
(49) Bartelmess, J.; Weare, W. W. *Dyes Pigm.* **2013**, *97*, 1−8.
(50) Bartelmess, J.; Weare, W. W.; Latortue, N.; Duong, C.; Jones, D. S. *New J. Chem.* **2013**, *37*, 2663.
(51) Trogler, W. C.; Stewart, R. C.; Epps, L. A.; Marzilli, L. G. *Inorg. Chem.* **1974**, *13*, 1564.
(52) Wenger, O. S.; Hanss, D. *Eur. J. Inorg. Chem.* **2009**, 3778.